2013 IEEE International Conference on Robotics and Automation (ICRA)
Karlsruhe, Germany, May 6-10, 2013

Design Principles for Highly Efficient Quadrupeds and Implementation on the MIT Cheetah Robot

Sangok Seok[1], Albert Wang[1], Meng Yee (Michael) Chuah[1], David Otten[2], Jeffrey Lang[2] and Sangbae Kim[1]

***Abstract*— In this paper, we introduce the design principles for highly efficient legged robots and the implementation of the principles on the MIT Cheetah robot. Three major energy loss modes during locomotion are heat losses through the actuators, losses through the transmission, and the interaction losses that includes all losses of the system interacting with the environment. We propose four design principles that minimize these losses: employment of high torque density motors, low impedance transmission, energy regenerative electronics and a design architecture that minimizes the leg inertia. We present the design features of the MIT cheetah robot as an embodiment of these principles. The resulting cost of transport (COT) is 0.51 during 2.3 m/s running, which rivals running animals in the same scale.**

I. INTRODUCTION

In the past several decades, roboticists have focused on using mobile robots for a variety of tasks. For untethered robots, energy efficiency is an essential aspect in practical applications. In recent years, stabilized locomotion of legged robots has been achieved, which have resulted in several successful biped and quadruped robots that can walk stably over flat ground as well as rough terrain. However, the energy efficiencies of these robots are still significantly worse than animals of similar masses. Total cost of transport (COT), a.k.a. specific resistance (SR), one of the most widely used measures of efficiency of legged animals and robots, is given by the power consumption divided by the weight times velocity [1]. Compared to animals, the COT of legged robots such as ASIMO (COT=2) and Boston Dynamics BigDog (COT=15) are significantly higher than animals with similar masses[2], [3]. Considering that electromechanical conversion (electricity to mechanical work) is much more efficient than biological energy conversion (fat to mechanical work), there seems to be substantial inefficiencies associated with current robot designs. The values for these robots are plotted with animal data in Figure 1.

To date there have been several research attempts to improve the efficiency robotic legged locomotion using two main approaches: employment of passive dynamics and series elastic actuators. The most successful example is the Cornell Ranger (COT=0.19) which utilizes the passive dynamics and trajectory optimization on a McGeer-style 4-legged biped [1], [4]. However, Ruina points out that the robot is designed specifically for energy efficiency and is not particularly practical [1]. This is because the robot sacrifices the versatility in function to maximize the employment of passive dynamics whereas BigDog and ASIMO are much more versatile. ASIMO is designed to be a multifunctional humanoid and BigDog can carry heavy loads over rough terrain so the comparison is not entirely fair. However, if the non-locomotive parts are removed, the robots would still have difficulty achieving the efficiency of either the Cornell Ranger or animals of similar scales.

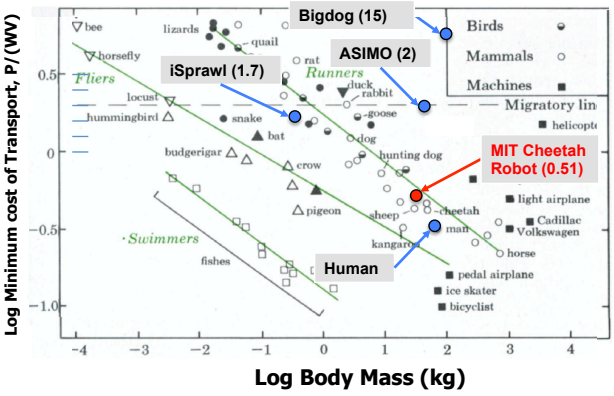

Fig. 1. Plot of Cost of Transport vs body weight of animals and selected robots. The three classes of animal locomotion (running, flying and swimming), occupy distinct regions of the plot. Adopted with permission from author of [2]

Another method of increasing energy efficiency is to use series elastic actuators. Series elastic is employed to utilize the high energy recovery of mechanical springs in work cycle in locomotion. iSprawl [5] shows a COT of 1.7 exceeding animal efficiency by utilizing series elastic actuation. The stiffness of series elastic spring is set for around 14Hz of stride frequency and the system becomes unstable in lower frequency running. To integrate series elastic actuation into the design of a general purpose robot is non-trivial as there needs to be ways of altering the mechanical stiffness and damping. This is usually achieved through the use of additional smaller actuators [6], which significantly increases complexity, weights and energy consumption. Other proposed approaches for efficiency include the employing of parallel springs [7] and optimizing swing leg retraction [8] for minimizing impact losses.

Although the energy efficiency is often addressed through optimal control of the robot, neither an actuator design

This work was supported by the Defense Advanced Research Program Agency M3 program

[1]Authors are with the Department of Mechanical Engineering, Massachusetts Institute of Technology, Cambridge, MA, 02139, USA , corresponding email: sangok at mit.edu

[2]Authors are with the Department of Electrical Engineering and Computer Science, Massachusetts Institute of Technology, Cambridge, MA, 02139, USA

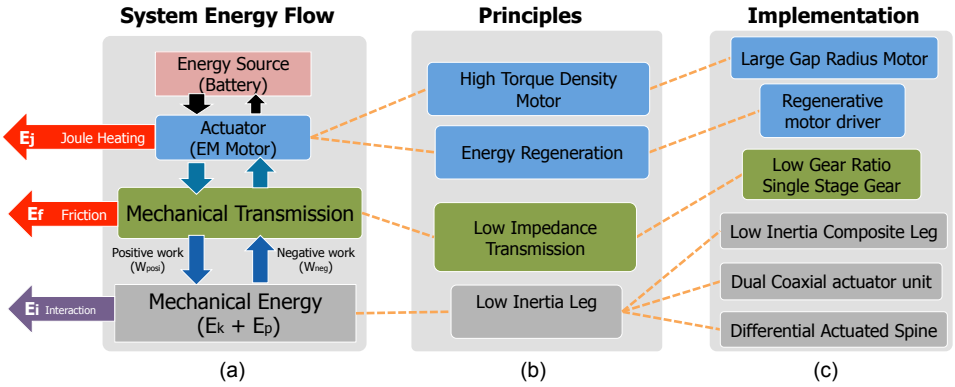

Fig. 2. (a) Energy flow diagram of the robot showing how the energy flow between the source and mechanical energy. Joule heating loss occurs at the motor, friction loss occurs in the mechanical transmission and interaction loss reduces the total mechanical energy. (b) Design principles for improve efficiency at the sources of energy loss. (c) Strategies for implementing the design principles for efficiency used on the MIT Cheetah Robot.

methodology nor comprehensive design principle has been suggested for minimizing energy loss. The electromechanical design not only governs the dynamic behavior of the robot but also characterizes the energy flow within the system during locomotion. In this paper, we will discuss the design principles for achieving high energy efficiency in quadrupedal robots by analyzing energy flow mechanisms within the entire system. The system comprises of energy source, actuators, mechanical transmission, and the interaction with the environment. Section II introduces the three major ways energy is lost in legged locomotion and how the proposed design principles can minimize the losses. Section III describes how we implemented the design principles in the MIT Cheetah robot. Section IV shows the gains in energy efficiency by comparing the cost of transport of the MIT Cheetah robot with biological runners and Section V discusses the conclusions we have drawn and our future work.

II. Design Principles for Efficiency

In this research, we used a comprehensive approach summarized in a diagram shown in Fig. 2(a). The leftmost column represents the energy flow of the robot. Locomotion over flat ground is an energy dissipative process, where there is no net change of mechanical energy (kinetic and potential) over a cycle. The energy reduction in energy source equals the sum of losses, which can be categorized into three losses.

The first loss is the heat loss at the force transducer. In an electromagnetic (EM) motor, this comprises of Joule heating, $E_j = I^2R$, and parasitic amplifier switching loss. The second is transmission loss, E_f. In a typical robot, this includes all losses through force transmission paths such as gear, belt friction loss and bearing friction. The third is the interaction loss. This includes all the losses caused at the interface between the system and the environment. Major sources of this loss in legged locomotion are the foot impacts and air drag. Inelastic impact loss for simple linear motion is given in (1) where ΔP is the impulse from impact, v^+ and v^- are the velocities of before and after impact respectively and m is the impact mass. A more detailed model for jointed robots can be found in [9]. The design of the robot needs to consider these factors to minimize overall loss.

$$\begin{aligned} mv^+ &= mv^- + \Delta P \\ E_i &= -\Delta E = -\tfrac{m}{2}[(v^+)^2 - (v^-)^2] \end{aligned} \tag{1}$$

We propose four design principles essential in the design of efficient robots. These principles shown in Fig. 2(b) directly address the three losses as denoted by the dotted lines.

A. High Torque Density Motor

This principle directly concerns the Joule heating of the motor by reducing the required electric current to provide adequate torque for the locomotion. If torque density[1] of motor doubles without changing other factors, the Joule heating E_j can be reduced to a fourth. Employment of gear transmission typically reduces E_j by increasing the overall torque density but it is associated with an increase in gear friction. This is not desirable for two major reasons: 1) gear mass required to deliver high torque is significant and cause reduction in total torque density of system, 2) increased mechanical impedance prevents the system from achieving highly dynamic proprioceptive force control [10] and increases friction losses, which compromises the efficiency of energy regeneration during negative work. Therefore, increasing the torque density of EM transducer is desirable for efficient locomotion without compromising the dynamics of the system.

B. Energy Regeneration

The principle of energy regeneration addresses the loss at the motor and drive electronics when braking the motor. In legged locomotion there are periods in each stride in which the leg does negative work [11]. Similar to regenerative braking in hybrid electric vehicles, it is desirable to recover that energy rather than dissipating it in dampers and brakes [12].

[1]Here torque density is defined as the continuous torque per mass. Assuming the thermal characteristics of the motors are similar, this metric is directly proportional to torque/Joule heating (τ/I^2R).

Another method of recovering energy involves the use of Series Elastic Actuation (SEA). An elastic element is placed between the actuator and the end effector that can temporarily store and release energy from ground contact. This can theoretically achieve higher efficiency with the actuator injecting a small amount of energy to account for impact losses.

We chose to employ proprioceptive force control [10] without series compliance and force sensors in order to achieve a wide range of leg impedances and high bandwidth control of large forces. The cost is additional transmission loss and energy conversion loss during energy recovery. However, if damping[2] is required, an electromagnetic damper in proprioceptive force control partially returns energy back to the source whereas mechanical damper dissipates entirely. Furthermore, any negative work can be recovered through regeneration of mechanical energy to electricity.

C. Low Impedance Transmission

A low impedance transmission allows the energy flow between the actuator and end effector in both directions. Ideal transmissions should be as 'transparent' as possible, not introducing any additional dynamics or power loss to the system [10].

Geared transmissions are usually paired with electric motors to amplify torque and reduce speed. Using gears significantly reduces the torque demands on the motors while increasing torque density. However, the addition of gearing adds reflected inertia, and reflected damping of the actuator to the output shaft, and the values are multiplied by the square of the gear ratio. Thus in highly geared systems, the reflected dynamics dominate and cause significant increase to overall impedance. SEA can lower the impedance of a highly geared transmission. However, the force as applied by the elastic element is difficult to control and would require energy consuming position feedback control on the actuator.

The major energy loss in the transmissions occurs as friction, either in the gears or bearings. These losses are dependent on force and can be modeled as a constant efficiency. Typically, each gearing stage introduces a constant percentage loss so the overall efficiency is taken as the efficiency of one stage to the power of the number of stages.

Gears also introduce another subtlety of asymmetric friction loss, in which friction loss in the torque amplification direction is smaller than when energy flows back towards the motor [13]. This effect in spur gears has not been fully investigated and the full gear model is ongoing work for the MIT Cheetah project [14]. A full gear interaction model is imperative for the simultaneous optimization of actuator and gear selection to minimize losses.

D. Low Inertia Leg

Equation (1) suggest two ways to mitigate impact losses: by minimizing the change in velocity at impact, and by reducing the impact mass. As the impact velocity is related to the relative velocity, it is necessary to control the retraction speed of the leg before impact on the ground [8]. Hence the only other alternative way to decrease the impact losses is to reduce the impact mass. A lower distal mass is desirable for minimizing impact. This also reduces the energy required to cycle the legs.

[2]Here, damping does not represent energy dissipative element but equivalent impedance.

III. Implementation of Design Principles on the MIT Cheetah Robot

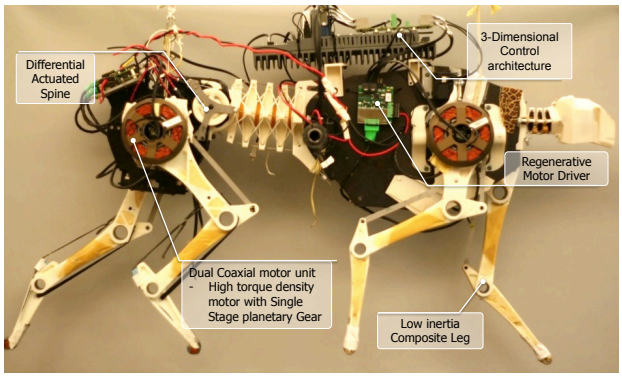

Fig. 3. Side view of the MIT Cheetah Robot showing design principles as implemented in hardware.

A. Large Gap Radius Motor

Seok et al. [10] showed that the radius of the gap between the motor stator windings and the permanent magnets on the rotor is a principal measure of motor performance. Without changing the mass of the motor, it is possible to increase several performance metrics by increasing the gap radius. Both the moment arm of the rotor and circumference of the rotor scale linearly with r_{gap} causing the overall torque output to scale by r_{gap}^2. However, the mass also scales by r_{gap} if we treat the stator windings and rotor magnets like thin wall structures, assuming that the pole-pair remains proportional to the thickness. Therefore overall torque per mass scales by r_{gap} while keeping all other motor parameters constant. Similarly, the torque per rotor inertia scales by r_{gap}^{-1} and the torque squared per power, a measure of efficiency calculated by $\frac{K_t^2}{R}$ in which K_t is the torque constant and R is the winding resistance, scales by r_{gap}^3.

We developed a custom designed three phase permanent magnet synchronous motor which is optimized for torque density [15] (gap radius: 48.5 mm, torque constant: 0.6 Nm/A, weight: 1kg, phase resistance: 0.6 Ω). The torque density of the motor is almost doubled compared with commercial motor currently used in the MIT Cheetah (Emoteq HT-5001, gap radius: 38.5 mm, torque constant of 0.3 Nm/A, weight: 1.3 kg, phase resistance: 0.354 Ω).

B. Motor Drive Electronics Design for Regeneration

The motor driver on the MIT Cheetah robot is a custom switching converter built from three half bridges, capable of driving a three phase motor at 60A from a 100V supply. The architecture of the motor driver is designed to act like

a bidirectional buck boost converter [16]. When energizing the motor, the motor driver bucks down the battery supply voltage to the desired phase voltages of the brushless motor [17]. In regenerative braking mode, the driver acts as a boost converter to step up the motor phase voltages to more than 100 VDC and recharge the batteries.

In the motor driver used on the MIT Cheetah robot, the motor driver commands voltages to each motor lead using PWM. If the duty cycle is D, then the voltage applied to the motor is Dv_{batt}. In the backward power flow direction, the motor driver is a boost converter and the stepped up voltage is $\frac{1}{D}v_{bemf}$ where v_{bemf} the back emf of the motor. If $\frac{1}{D}v_{bemf} > v_{batt}$ then the energy from braking the motor recharges the batteries.

A simple experiment was performed to verify regeneration during negative work. The Cheetah robot was lifted and dropped onto one leg, while commanding a fixed position held by a virtual spring with proportional gain of 5 kN/m and damping of 100 Ns/m. The data from the experiment shown in Fig. 4 show that the batteries are indeed recharged. The voltage of the battery line shown in Fig. 4(a) experiences a voltage spike from the boosted motor voltage and Fig. 4(b) clearly shows current flow back into the battery. Fig. 4(c) accounts for the mechanical work done by the motor, the amount of the Joule heating in the motor windings and the power consumption at the batteries. 63% of the negative mechanical work done by the motors is recovered by the batteries in the experiment.

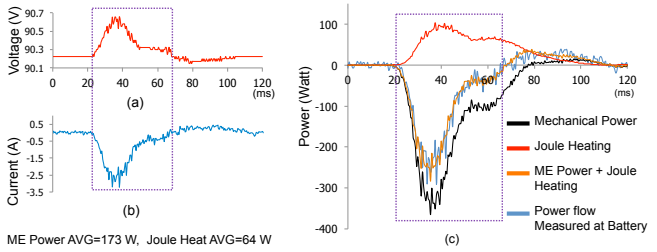

Fig. 4. (a) Voltage of the battery supply line during the regeneration experiment. (b) Current flowing out of the batteries during the regeneration experiment. (c) The mechanical power, Joule heating dissipation and battery power measured during experiment. Note that 63% of the negative mechanical work done by the motors is recovered by the batteries in the experiment.

C. Low Gear Ratio Transmission

The MIT Cheetah robot uses a custom designed, single stage of planetary gearing with a gear ratio of 5.8:1 on each motor, the largest ratio that can be obtained in a single stage. The relatively low ratio reduces the contribution of reflected actuator dynamics on the impedance of the transmission output, and the number of gear stages is reduced to one to minimize cascading gear loss. However, the value is not optimized due to the lack of a detailed loss model.

The friction of the mechanical transmission was measured to determine its effect on proprioceptive control [10]. A diagram of the setup is shown in Fig. 5(a). The leg was subjected to a compression and decompression cycle applied externally by a linear material testing device. The motors were commanded to act as a virtual spring to the resist the compression. We measured the expected output force from the motor current and compared it to the force at the foot measured by a force sensor. The two forces are shown in Fig. 5(b) and the transmission loss is modeled as a force dependent coulomb loss acting against the direction of travel. The resulting friction coefficient is 0.095, equivalent to 9.5% power loss.

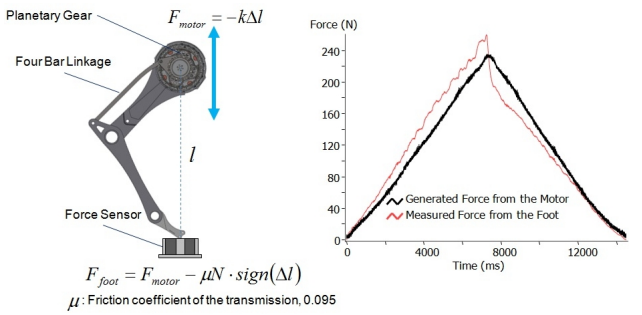

Fig. 5. (a) The experimental for determining the loss in the mechanical transmission. The force at the foot is calculated using the torques applied by the motors and compared against a force sensor under the foot. (b) Experimental data showing the difference between the expected the force on the foot as generated from the motors and the actual force measured.

D. Composite Leg

To be conducive for high speed running, a quadruped robot needs to have a high stride frequency and low duty factor [18]. To increase the stride frequency, one can either increase the actuator capacity or decrease the leg inertia. But increasing the actuator capacity would also increase the actuator mass. This would cause the effective ground reaction force to increase during running, which would then require that the robot have stronger legs to resist the higher bending moment. Another way is to decrease the individual leg inertias of the robot. Towards this goal, the tendon-bone co-location architecture was implemented in the MIT Cheetah in order to reduce the inertia of the legs [19]. It is hypothesized by biologists that in human legs experiencing ground impact, the bones carry only compressive loads while the muscles, tendons and ligaments carry the tensile loads [20]. This distribution makes effective use of the relative advantages of each biological material to achieve a strong but light structure. By having this synergetic arrangement of bones and tendons, the human leg is also better able to resist bending moments incurred during ground impact. To achieve this same tendon-bone co-location architecture, a Kevlar tendon was integrated into the design of the MIT Cheetah leg, linking the foot to the knee. Experiments show that this architecture reduces the stress experienced by the bone during stride by up to 59%. The bone structure of the robot leg also draws inspiration from biological structures. This is done by having a rigid and light polyurethane foam-core for the leg covered in a high stiffness polyurethane resin to form a composite with high strength but low inertia. Further

details on the tendon-bone co-location design architecture and experiments performed on the robot leg can be found in the paper by Ananthanarayanan et al. [19].

E. Dual Coaxial Motor Design

In traditional serial link robots, the actuators are usually located at the joints. This simplifies the control of the robot but increases the inertia of the distal links. In the MIT Cheetah, the aim is to lower the rotational inertia of the leg. Hence, the two motors are placed co-axially in the shoulder. One motor actuates the shoulder joint while the other actuates the knee through the use of a four bar steel linkage. The center of mass is 45 mm from the center of rotation [10].

F. Differential Actuated Spine

In the case of the MIT Cheetah, a flexible spine was implemented to explore the possible energetic benefits it might bring to high speed running. We specifically design the spine actuation mechanism to select among rigid, passive, and actuated mode. The spine is made up of rings of polyurethane rubber sandwiched by spine vertebrae segments. Through the innovative use of a differential, the spine is actuated without the necessity of an extra actuator, which would require a large torque. Instead, the motions of the two rear legs are coupled to the motion of the spine through the differential as seen in Fig. 6. In the actuated mode, the polyurethane rubber ring can store elastic energy and return it during galloping.

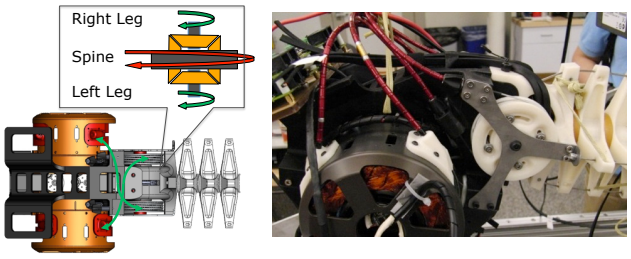

Fig. 6. Spine Differential Cabling. As the MIT Cheetah runs, the steel cables couple the motions of the rear legs to the motions of the spine in the sagittal plane. The colors indicate how the cabling couples each leg to the differential input shafts which then outputs to the center drum to actuate the spine.

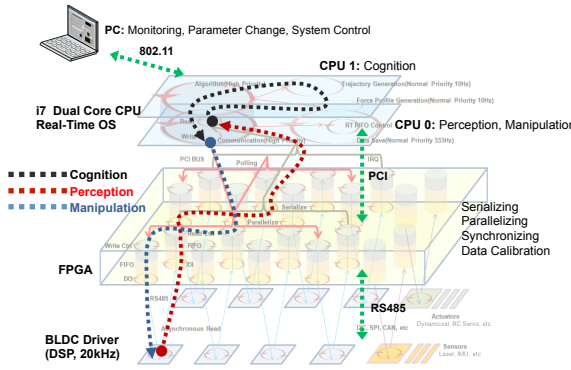

Fig. 7. Multi-layered, 3D programming structure used for the control of the robot.

IV. Experiment

A. High Speed Control System Architecture

A novel multi-layered '3-Dimensional Control System Structure' was designed to manage the complicated data flows. The control system structure comprises of four layers: Real-Time controller, FPGA, Motor driver, and the PC. Perception data flows from the Brushless Direct Current (BLDC) motor driver to the Real-Time controller through the FPGA layer. This information then gets processed by the Real-Time CPU which then sends the appropriate manipulation data back to the motor driver. The NI cRIO-9082 houses both the FPGA layer and the Real-Time controller and is programmed using LabVIEW. The motor driver microcontroller (Microchip dsPIC30F6010) handles the current control of one BLDC motor at 20 kHz. RS-485 is used for the communications protocol. The FPGA layer (Spartan-6 LX150) collects the asynchronous data from eight motor drivers and then synchronizes and serializes all the data before sending data to the Real-Time controller. It also receives current commands for the motor drivers from the Real-Time controller and sends to each motor driver simultaneously. The Real-Time controller (i7 dual-core 1.33 GHz) is made up of two cores (CPU 0 and CPU 1). CPU 0 receives the calibrated data from the FPGA layer and sends back the current commands in a high priority loop that runs at 4 kHz. Data logging occurs in a normal priority loop in the same CPU with 1 MB/s writing speed. CPU 1 contains all the algorithms used to compute the forward kinematics and Jacobian matrices in a high priority loop (4 kHz). A normal priority loop also does the trajectory generation and force profile generation. The PC is used for monitoring and controlling the system wirelessly through the 802.11 protocol.

B. Efficiency of running

To measure the efficiency of the MIT Cheetah robot, we ran it at 2.3 m/s on a treadmill. The robot was constrained in the sagittal plane to prevent roll and yaw, but was free in pitch, vertical translation and fore-aft translation. The legs were commanded with a trot trajectory with an impedance feedback controller. For safety, the batteries were not located on the robot, but a 3 kg mass was attached to the cheetah body to simulate the weight.

Fig. 8 shows power consumption during 2.3 m/s running. We measured the voltage and current of the battery as well as the current and encoder position of the motor. Using the measurements obtained, mechanical power, Joule heating and battery power were calculated using the equations in Eq. 2. The curves of 'Power Consumption Measured at Battery' match up with the sum of 'Mechanical Power + Joule Heating', which indicates that the instrumentation is correctly calibrated.

$$\begin{aligned} \text{Mechanical Power} &= \textstyle\sum_{8 \text{ motors}} \tau \times \omega \\ &= \textstyle\sum_{8 \text{ motors}} K_t \times I_{motor} \times \omega \\ \text{Joule Heating} &= \textstyle\sum_{8 \text{ motors}} I_{motor}^2 R \\ \text{Battery Power} &= V_{battery} \times I_{battery} \end{aligned} \tag{2}$$

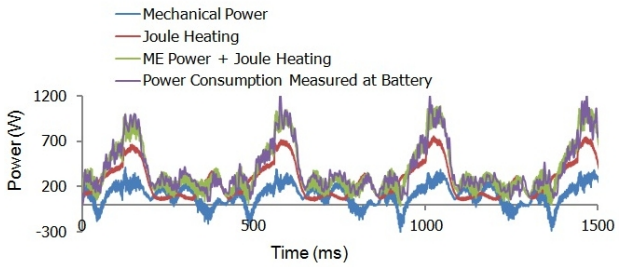

Fig. 8. Power consumption measurements during 2.3 m/s running

Table I shows several attributes of the power consumption in the MIT Cheetah Robot. Of the 377 W consumed, 256 W is lost in Joule heating, 100 W of mechanical power is produced by the actuator, 21 W is the power dissipated by 8 motor drivers and also includes hysteresis losses in the polymeric legs. Joule heating (68% of all electrical power) is by far the predominant mode of power consumption.

TABLE I

MIT CHEETAH POWER CONSUMPTION VALUES DURING 2.3 M/S RUNNING

Total Power	Joule Heating	Mechanical Power	Electronics Dissipation, etc	COT	with 3Kg Battery (465Whrs)	
					Running Time	Distance
377 W	256 W (68%)	100 W (26.5%)	21 W (6.5%)	0.51	1.23 Hrs	11.07 km

Fig. 1 shows the COT of animals in nature as well as man-made vehicles. The COT of representative robots are overlaid [5], [3] to compare the metabolic energy consumption of animals with the overall power consumption of mobile robots. For animal data, the three classes of locomotion (runners, fliers, and swimmers) occupy distinct regions of the plot of COT versus body mass. The MIT Cheetah has a mass of 33 kg and a COT of 0.51 which is on the same level as other biological runners of similar mass.

V. CONCLUSIONS

We have successfully demonstrated high efficiency legged robot locomotion using the four major design principles highlighted in this paper. The MIT Cheetah is able to achieve a cost of transport that matches running animals in nature. From the analysis of energy loss in the components of the system, we conclude that the motor resistance is the major source of power loss in the robot. We have developed a new custom motor that has 1.8 times the torque constant and 1.6 times the phase resistance of the motor currently used on the robot. Once implemented on the MIT Cheetah robot, we expect to reduce COT to 0.33 which is between the efficiency of runners and fliers in nature.

ACKNOWLEDGMENT

Thanks to Vance Tucker, Professor Emeritus at Duke University for his early investigation of animal locomotion that have inspired modern robots to strive towards the efficiencies found in nature. Thanks to National Instruments for hardware support.

REFERENCES

[1] P. Bhounsule, J. Cortell, and A. Ruina, "Design and control of ranger: An energy-efficient, dynamic walking robot," in *CLAWAR 2012 - Proceedings of the Fifteenth International Conference on Climbing and Walking Robots and the Support Technologies for Mobile Machines*, July 2012, pp. 441–448.

[2] V. A. Tucker, "The energetic cost of moving about: Walking and running are extremely inefficient forms of locomotion. much greater efficiency is achieved by birds, fishand bicyclists," *American Scientist*, vol. 63, no. 4, pp. pp. 413–419, 1975.

[3] A. Ruina. (2012, September) Cornell ranger 2011, 4-legged bipedal robot. [Online]. Available: http://ruina.tam.cornell.edu/research/topics/locomotion_and_robotics/ranger/Ranger2011/

[4] R. Tedrake, T. Zhang, M. Fong, and H. Seung, "Actuating a simple 3d passive dynamic walker," in *Robotics and Automation, 2004. Proceedings. ICRA '04. 2004 IEEE International Conference on*, vol. 5, april-1 may 2004, pp. 4656 – 4661 Vol.5.

[5] S. Kim, J. Clark, and M. Cutkosky, "isprawl: Design and tuning for high-speed autonomous open-loop running," *The International Journal of Robotics Research*, vol. 25, no. 9, pp. 903–912, 2006.

[6] S. Wolf and G. Hirzinger, "A new variable stiffness design: Matching requirements of the next robot generation," in *Robotics and Automation, 2008. ICRA 2008. IEEE International Conference on*, may 2008, pp. 1741 –1746.

[7] S. K. G. Folkertsma and S. Stramigioli, "Parallel stiffness in a bounding quadruped with flexible spine," in *IEEE/RSJ International Conference on Intelligent Robots and Systems*, October 2012.

[8] M. Haberland, J. Karssen, S. Kim, and M. Wisse, "The effect of swing leg retraction on running energy efficiency," in *Intelligent Robots and Systems (IROS), 2011 IEEE/RSJ International Conference on*, sept. 2011, pp. 3957 –3962.

[9] I. Walker, "The use of kinematic redundancy in reducing impact and contact effects in manipulation," in *Robotics and Automation, 1990. Proceedings., 1990 IEEE International Conference on*, may 1990, pp. 434 –439 vol.1.

[10] S. Seok, A. Wang, D. Otten, and S. Kim, "Actuator design for high force proprioceptive control in fast legged locomotion," in *IEEE/RSJ International Conference on Intelligent Robots and Systems*, October 2012.

[11] A. Ruina, J. Bertram, and M. Srinivasan, "A collisional model of the energetic cost of support work qualitatively explains leg sequencing in walking and galloping, pseudo-elastic leg behavior in running and the walk-to-run transition," *Journal of Theoretical Biology*, vol. 237, no. 2, pp. 170 – 192, 2005.

[12] M. Yoong, Y. Gan, G. Gan, C. Leong, Z. Phuan, B. Cheah, and K. Chew, "Studies of regenerative braking in electric vehicle," in *Sustainable Utilization and Development in Engineering and Technology, 2010 IEEE Conference on*, nov. 2010, pp. 40 –45.

[13] M. Dohring, E. Lee, and W. Newman, "A load-dependent transmission friction model: theory and experiments," in *Robotics and Automation, 1993. Proceedings., 1993 IEEE International Conference on*, may 1993, pp. 430 –436 vol.3.

[14] A. Wang, "Directional Impedance of Geared Transmissions," Master's thesis, Massachusetts Institute of Technology, 2012.

[15] N. Farve, "Design of a low-mass high-torque brushless motor for application in quadruped robotics," Master's thesis, Massachusetts Institute of Technology, 2012.

[16] F. Caricchi, F. Crescimbini, F. Capponi, and L. Solero, "Study of bi-directional buck-boost converter topologies for application in electrical vehicle motor drives," in *Applied Power Electronics Conference and Exposition, 1998. APEC '98. Conference Proceedings 1998., Thirteenth Annual*, vol. 1, feb 1998, pp. 287 –293 vol.1.

[17] D. Torres and P. Heath, "Regenerative braking of bldc motors," Microchip Technology Inc., Tech. Rep.

[18] L. Maes, M. Herbin, R. Hackert, V. Bels, and A. Abourachid, "Steady locomotion in dogs: temporal and associated spatial coordination patterns and the effect of speed," *Journal of Experimental Biology*, vol. 211, no. 1, pp. 138–149, 2008.

[19] A. Ananthanarayanan, M. Azadi, and S. Kim, "Towards a bio-inspired leg design for high-speed running," *Bioinspiration and Biomimetics*, vol. 7, no. 4, p. 046005, 2012.

[20] K. Rudman, R. Aspden, and J. Meakin, "Compression or tension? the stress distribution in the proximal femur," *BioMedical Engineering OnLine*, vol. 5, no. 1, p. 12, 2006.